Time-of-flight imaging of hyperpolarized gas flows in the human airways at true temporal resolution lower than 10 ms

X. Maître[1], S. Besse[1], F. Mauconduit[1], V. Senaj[1], E. Durand[1], L. Darrasse[1], and J. Bittoun[1]

[1]Unité de Recherche en Résonance Magnétique Médicale, CNRS (UMR8081) - Université Paris-Sud, Orsay, France

Purpose

Tracking down the gas flow in the human lungs during an inhalation faces the limited temporal resolution of available imaging techniques. Fast EPI [1] and interleaved spiral [2] sequences were introduced to respectively reach 40 and 10 ms as pseudo-temporal resolution by means of a sliding window. Arrival times in the distal airways could be measured but true temporal resolutions rather lay in the 200 ms range [3] whereas the averaged time for the gas to propagate throughout a bronchus segment during a normal inspiration is about 17 ms. A more recent multi-echo SSFP sequence led to a 51 ms separation between subsequent images [4]. Yet the gas propagation through the upper and proximal airways has remained inaccessible. Following the original work for blood velocity assessment [5], we achieved here a true 10 ms temporal resolution and we measured gas velocities and flow patterns of a 10 s steady inspiration, *in vitro*, through airway casts and, *in vivo*, in the nasal airways.

Material and methods

The motion of helium-3 spins was captured in airways by time-of-flight measurements on a set of N=16 to 32 images in a similar fashion as in [5]. First, a π/2 RF pulse followed by a crusher gradient pulse is applied to suppress any initial total magnetic moment present in the imaging site. Then acquisition of the N images was interlaced in a 2D gradient-echo sequence with a variable flip angle $\alpha=\arctan(1/N\text{-}n)^{1/2}$ where n is the image index. Thereof, the signal originating from the gas propagation front remains constant throughout the whole acquisition while the total magnetic moment present in the coil is fully utilized and reset at the end of every N^{th} RF pulse letting the system ready for acquisition of the subsequent Fourier line N-series. The steady gas inflow in the observed airways provides new polarized helium-3 that has flowed therein for the n^{th} image during n×TR. Therefore, at a given phase-encoding step, the lines of the N Fourier planes are consecutively scanned and the resulting N images are snapshots of the gas, which can be sequentially visualized as a movie with a 1/TR frame rate per second.

The cine-acquisition sequence was implemented with a FOV of 210×210 mm^2, a matrix of 64×64, a bandwidth of 155 Hz/pixel, TR/TE=9.4/2.9 ms, a 25% echo asymmetry and a total acquisition time of 9.5 s for N=16 images on a 0.1 T MR-unit (Sopha-Imaging, France) retuned to the helium-3 frequency at 3.29 MHz and equipped with a third-party digital NMR console (Tecmag, Houston, Texas). The gradient system was stabilized and accelerated to reach 14 $mT\cdot s^{-1}$ within 800 µs [6]. A pair of curved Helmholtz coils, with a quality factor of 200, was used in transmit/receive mode. *In vitro* experiments were carried out on phantoms of proximal and upper airways materialized by rapid prototyping after a segmentation of the airway geometries taken from two subjects' CT thoracic lung scans (Figures d. and e.). In the bronchial tree phantom, the dose was administered by pressured helium-4 injection through the input trachea at a constant flow rate. In the nasal airway phantom, the hyperpolarized helium-3 dose was administered through the nostrils by inspiration from the output trachea by a vacuum pump at a constant flow rate. The corresponding input and output flows were monitored during the signal acquisition by a mass flowmeter (AWM700; Honeywell International Inc., Morristown, New Jersey). *In vivo* experiments were achieved on the upper airways of a volunteer by mere steady inspiration of hyperpolarized helium-3 through the nostrils over the 10 s acquisition time (N=16). For each acquisition, 70 mL of helium-3, polarized up to 20%, was produced by metastability exchange optical pumping [7] and completed by helium-4 up to 500 mL before being transferred to the imager *via* a Tedlar® bag.

The amplitude images were masked out at three times the noise value. They were then weighted by a coil sensitivity map obtained from a homogeneous helium-3 phantom [8] and finally normalized to their maximum. The highest gas velocity in the proximal airways was inferred down to the second bronchial generation by following the propagation front of the gas signal and by calculating the ratio of its displacements between serial images and TR. The propagation front was defined as the end pixel found in the airway on the processed image. Flow rates within the airways were derived for their given mean cross sections while assuming a Poiseuille flow for which the mean velocity is half the maximum. In the upper airways, velocities were inferred from the sets of images.

Results

In vitro input flow of the bronchial tree was (521±9) $mL\cdot s^{-1}$. Over the unmasked regions of the N images, the maximal signal to noise ratios ranged between 11 and 116. Only 8 of the 32 and 16 acquired images are presented for the two phantoms on Figure a. and b. From the first eight images that depict the tracheal gas motion in the bronchial tree (up to the 2nd image on Figure a.), an inter-image mean displacement of (12.1±1.6) mm yields a mean flow rate of (523±13) $mL\cdot s^{-1}$. From images 9 to 16, flows of (385±25), (176±9), and (172±12) $mL\cdot s^{-1}$ were processed in generations 1.1, 1.2, and 1.1.2 (Figure a.). From the first seven images, maximal velocities from 0.3 to 2.5 $m\cdot s^{-1}$ were measured in the phantom nasal cavity while the total mean flow throughout the larynx was (204±67) $mL\cdot s^{-1}$. *In vivo* recorded maximal velocities were between 0.3 and 1.6 $m\cdot s^{-1}$ in the nasal cavity and they reached 2.5 $m\cdot s^{-1}$ in the pharynx (Figure c.).

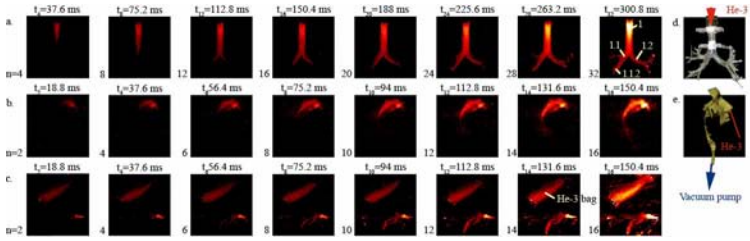

Figure: Reduced set of acquired cine-images *in vitro* (a) on a bronchial tree – every 4th image is presented – (b) on a nasal airway phantom and (c) *in vivo* in the nasal airways – every 2nd image is presented.

Discussion and conclusion

The flow in the trachea of the phantom matched the measured input flow rate. The total flow was conserved between the trachea and the first bronchial generation. Moreover, the flow patterns derived from the set of images from the bronchial tree are close to former CFD simulations and phase contrast measurements performed on the same phantom [9]. The slight discrepancies partly result from the assumption of a Poiseuille flow that cannot be totally fulfilled in the considered bronchi. More regional velocity and flow maps were also obtained – as in the nasal cavity here. The spatial resolution of such maps is given by the displacement between two images, which is in the millimeter scale. The flow measurement is degraded in larynx by lack of signal around the restriction of the vocal cords. On *in vivo* images, the helium-3 delivery bag outside the coil was imaged with aliasing. Motion artifact also appeared but both effects could be avoided in the future by proper positioning of both the bag and the subject's head.

Such time-of-flight measurements give accurate and robust means to measure gas flow maps within the human airways during a single steady inhalation. Slice selection could be implemented to reach lower region of the human lungs. The bias introduced by the image projection could be circumvented by correlating the missing dimension and the signal dynamics. Besides, it should be possible to characterize the projected velocity profile by following propagation fronts at different signal levels, thus following different velocity classes. Hence, the mean velocity value could be directly inferred. The mean cross sections of the cast airways were known here but they could also be estimated on the last image of the set with the assumption of circular airways. This approach provides true temporal resolutions never reached so far with hyperpolarized gases. It would highly benefit from parallel acquisition with a coil array since both the acquisition time and the RF depolarization would then be reduced such that temporal resolution would be consequently improved and spatial gas propagation, increased. Here, it was already possible to track a very light dephasing of a tenth of ms in the propagation of the gas in the two bronchi of the first generation. It could be advantageously applied to small animal imaging where timing is even more critical and where a 3D acquisition could be sought over several respiratory cycles by continuous helium-3 administration. Finally, the variable-angle cine-method proposed here for helium-3 would be profitable to proton investigations and more generally to any investigations with prepared magnetization, which include carbon-13.

References: **1**. Saam *et al.*Magn Reson Med 1999;42(3):507-514 **2**. Salermo *et al.* Magn Reson Med 2001;46(4):667-677 **3**. Gast *et al.* Invest Radiol 2002;37(3):126-134, Dupuich *et al.* Magn Reson Med 2003;50(4):777-783 **4**. Manjunath Pai *et al.* ISMRM 2006:866 **5.** Miraux *et al.* Magn Reson Med 2006;56(3):469-473 **6.** Senaj *et al* Meas Scien Rev 2003;3(3):61-64 **7.** Choukeife *et al.* ISMRM 2003:1391 **8.** Maître *et al.* ISMRM 2006:1303 **9.** de Rochefort *et al.* Magn Reson Med 2006;55(6):1318-1325

Acknowledgments: The authors would like to thank Sylvain Miraux for the fruitful discussion they had, Redouane Fodil, Bruno Louis, and Daniel Isabey for their kind and constant support.